Department of Physics, IIT Delhi

Course Code : PYD561
Semester - II, 2022-23

Plasma Mirrors

Kulwinder Kaur (2021PHS7190)
Harikesh Kushwaha (2021PHS7181)

Adviser: Prof. Vikrant Saxena

Signature of the first student: .....

Signature of the second student: .....

Signature of the adviser: .....

1 Introduction And Motivation

The study of how light interacts with matter at extremely high-intensity levels, known as Ultra High Light Intensity (UHLI), has garnered significant interest. The main objective is to achieve high-intensity levels, such as the experimental attainment of laser intensities of around $10^{23} W/cm^{-2}$ using the CoReLS petawatt (PW) laser[1], which can provide access to novel physical regimes. At these ultra-high intensities, laser-plasma interactions lead to various nonlinear processes, including the widely studied high harmonic generation[2]. High harmonics have various applications, such as ultrafast quantum information processing, attosecond sources, and all-optical mapping of the electronic band structure. One method of generating high harmonics involves using plasma, which is discussed in this article.

When a laser pulse is incident upon plasma, it reflects if the density of plasma is high, forming PM. Upon reflection from plasma the laser field, because of pondermotive force, propels a relativistic oscillation of the PM which results in periodic temporal compression of the reflected field. These oscillations result in the generation of high harmonics of the incident laser frequency.[3] Experimental demonstrations have shown the generation of high harmonics up to the 141st order of Nd glass laser[4], 109th order of Ti sapphire laser[5], and 37th order of krypton fluoride laser[6].

To begin, a concise explanation of high harmonic generation is provided, including its occurrence in both gases[7][8][9] and plasma[10][11][12][13][14]. The focus then shifts to the generation of harmonics of an incident laser pulse through interaction with an overdense plasma layer at a step boundary, under the influence of a high-intensity laser pulse. The impact of the laser pulse envelope, super-Gaussian (SG) with different rank p, on the resulting high harmonics is explored. Previously, simulations involving normal laser incidence revealed that only odd harmonics were generated. However, in the present report, various polarization and oblique incidences of laser light are simulated, resulting in the generation of both odd and even harmonics. For this, fully relativistic particle-in-cell simulations are performed using *EPOCH*[15].

2 Theoretical Background

High harmonic generation (HHG) is an optical phenomenon that involves nonlinear processes wherein laser light frequency is converted into multiple integer multiples. When atoms and molecules are exposed to intense laser fields, typically in the near-infrared range, harmonics of extremely high orders are produced.[9] We'll start with a brief overview of the theory of HHG in gases, followed by a discussion of HHG in plasma.

2.1 HHG in Gases

HHG in gases occurs when an intense laser pulse interacts with gases. Three types of ionization occur, depending on the frequency and intensity of the light. If the energy of the photon is greater or just equal to the atom ionization potential, then photon ionization occurs. However, if the energy of the laser is less than the atom ionization potential then multiphoton ionization and tunneling ionization occur. Multiphoton and tunneling ionization are determined by the laser frequency ω, the amplitude of the laser field strength F, and the atomic ionization potential I_p. In the multiphoton limit, the ionization rate follows a power law, while in the tunneling limit, the ionization rate increases exponentially with field strength. The adiabaticity parameter, given by

$$\gamma = \Omega \sqrt{2I_p/F} \tag{1}$$

determines the boundary between multiphoton and tunneling ionization, with high values corresponding to multiphoton ionization and low values to tunneling ionization. To be precise, $\gamma^2 \gg 1$ corresponds to multiphoton ionization and $\gamma^2 \ll 1$ to tunneling ionization.[8]

2.1.1 Three Step Model

In the three-step model, the electron is initially treated quantum mechanically as it tunnel ionizes from the parent atom but then its subsequent dynamics are treated classically. The HHG occurs in three steps:

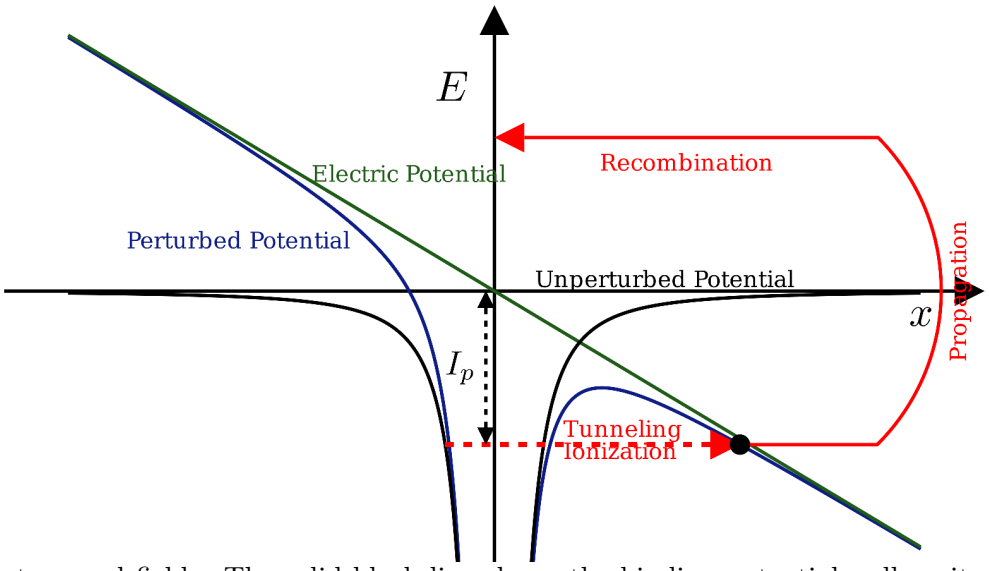

Figure 1: Three steps and fields. The solid black line shows the binding potential well on its own. The green line is the potential due to the laser field and the solid blue line shows the potential created by the instantaneous laser field and the binding potential well.

1. **Tunnel ionization** The laser field, which we have assumed to be linearly polarized along the x-axis, gives a potential in the form of $\hat{V}_L(t) - xFcos(\omega_L t)$, that is, the potential is proportional to $-x$. This is drawn in figure 1 as the green line. When this potential couples with the original potential well (in the black line), the potential is deformed (the blue line), called barrier suppression. Electron tunnels through this potential well.

2. **Free propagation in the presence of the field** Once the electron tunnels, it is assumed to be born into the vacuum with zero initial velocity. It is subsequently accelerated by the laser beam's electric field. Half a cycle after ionization, the electron will reverse direction as the electric field changes its direction, and will accelerate back toward the parent nucleus.

3. **Recollision and recombination** Next, the electron will collide with the nucleus which is the recombination process. During recombination, while the electron returns to its ground state, it can emit radiation of frequency that are multiple of the laser intensity. This is how high harmonics are generated.

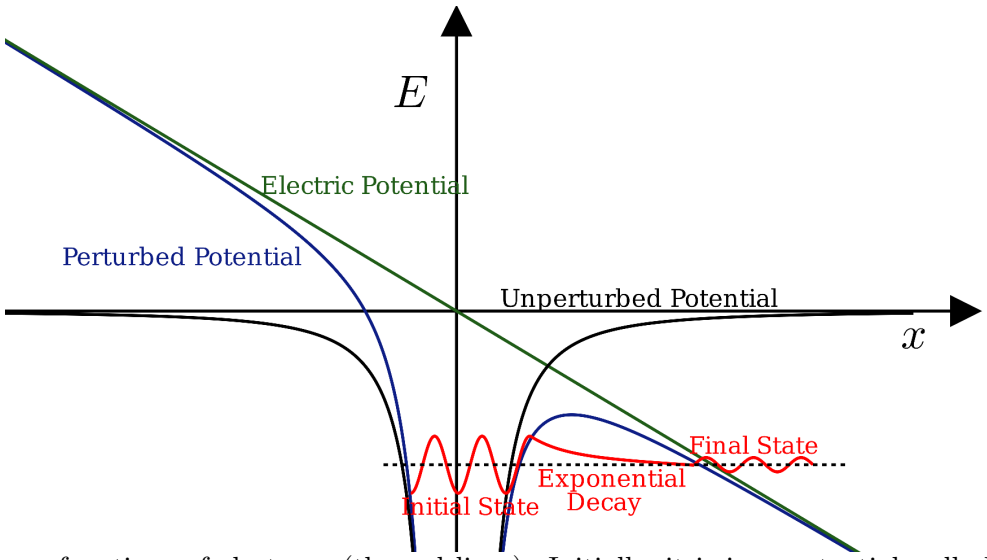

Figure 2: The wave functions of electrons (the red lines). Initially, it is in a potential well. While tunneling, the wave function decay exponentially. After the electron has tunneled through the barrier, it behaves like a free particle with a wave function specified by a smaller amplitude.

2.2 HHG in Plasma

The spectrum from HHG consists of several of integer harmonics of the incident laser pulse (with their intensities decreasing), followed by a plateau where the harmonic intensity is nearly constant over many orders and a sharp cutoff. Several of models and theories have been proposed explaining this power law and cutoff. Bezzerides et al.[10] gave the first model way back in 1983. Their model was based on the relativistic equation of motion and hydrodynamics approximation. They found a cutoff frequency as

$$n_{\max}^2 = n_p/n_c \tag{2}$$

where n_p is the plasma density and n_c is the critical density. They demonstrated that the principal source of high-harmonic emission is the strong non-linear restoring force that exists when resonant absorption occurs in a highly steep density profile. However, this model was not able to explain the plateau region as well as the fact that we get harmonics that are much higher than the cutoff frequency given by Eq. 2.

2.2.1 Oscillating Mirror Model

The idea behind this model is that the incident laser field then drives a periodic oscillation of the plasma mirror surface, at relativistic velocities. This relativistic oscillating mirror induces a periodic Doppler effect on the reflected field which is responsible for HHG. The model assumes that the duration of the light pulse is sufficiently short so that the motion of the ions may be neglected. The ions are treated as a fixed positive background charge. Also, the model neglects the details of the changes in the electron density profile and represents the collective electronic motion by the motion of the boundary of the supercritical region. This boundary represents an effective reflecting surface performing an oscillatory motion, the oscillating mirror. Using these assumptions, we follow von der Linde et al.[11] to derive the spectrum of HHG. First, we show that the HHG can be understood as a phase modulation due to the moving mirror.

For this, neglecting for a moment retardation affects the phase shift of the reflected wave resulting from a sinusoidal displacement of the reflecting surface in the z-direction:

$$s(t) = s_0 \sin(\omega t)$$

is given by

$$\phi(t) = (2\omega_0 s_0/c)\cos\alpha \sin\omega_m t$$

where α is the angle of incidence and ω_m is the mirror frequency (modulation frequency). The electric field of the reflected wave is given by

$$E_R \propto e^{-i\omega_0 t} e^{i\phi(t)} = e^{-i\omega_0 t} \sum_{n\to-\infty}^{n\to-\infty} J_n(\chi) e^{-in\omega_m t} \tag{3}$$

where $J_n(\xi)$ is the Bessel function of order n and

$$\chi = \frac{2\omega_0 s_0 \cos\alpha}{c} \tag{4}$$

The reflecting surface performs a periodic motion at a frequency $2\omega_0$, or a superposition of ω_0 and $2\omega_0$, depending on the polarization and angle of incidence of the incoming light. Thus, the modulation frequencies provided by the mirror motion are $\omega_m = \omega_0$ and/or $\omega_m = 2\omega_0$. The key point is that this type of modulation produces sidebands representing even and odd harmonics of the fundamental frequency ω_0 . These ideas suggest an interpretation of high-order harmonic generation from a plasma-vacuum interface as a phase modulation from a periodically moving reflecting surface.

2.2.1.1 p- and s-Polarization

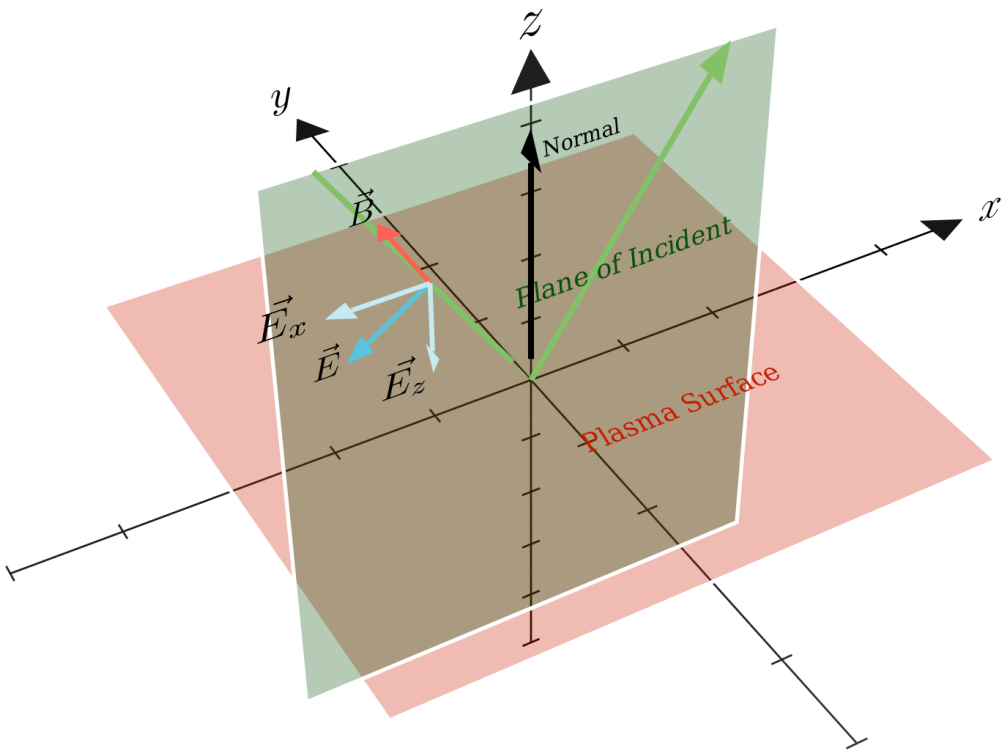

Figure 3: p-polarization. The electric and magnetic fields of the incident light are, respectively, parallel and perpendicular to the plane of incidence. The electrons move in the plane of incidence.

- **p-Polarized Light**: The electric and magnetic fields are, respectively, parallel and perpendicular to the plane of incidence. The electrons move in the plane of incidence. The electron boundary is driven at frequencies ω_0 and $2\omega_0$, because both the transverse and the longitudinal component of the electron velocity contribute to the motion of the boundary. It follows that in this case both even and odd harmonics with p-polarization are generated. See Fig. 3.

- **s-Polarized Light**: The electric field is parallel to the plasma-vacuum interface. The electrons move in a plane perpendicular to the plane of incidence. In this configuration only the longitudinal component contributes, while the transverse component of the electron motion is ineffective. The normal motion of the mirror is driven at one frequency only, $\omega_m = 2\omega_0$. It follows that the reflected light is composed of s-polarized odd harmonics and p-polarized even harmonics. See Fig. 4.

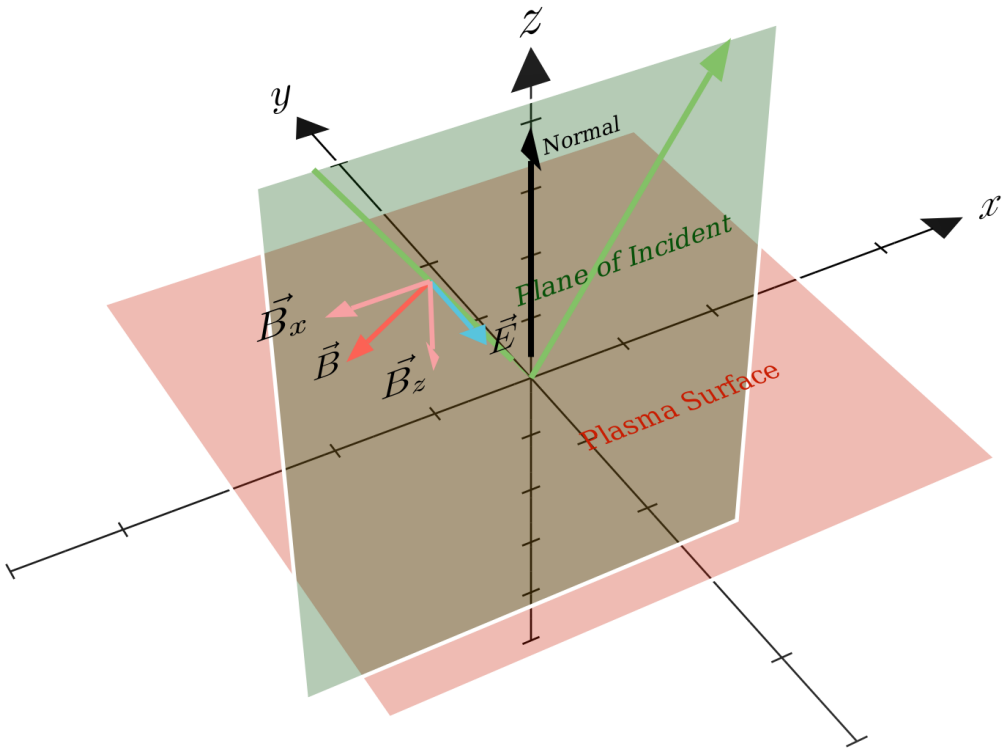

Figure 4: s-polarization. The electric field is parallel to the plasma-vacuum interface. The electrons move in a plane perpendicular to the plane of incidence.

Table 1: Polarization Selection Rule

	s-polarized Harmonics	**p-polarized Harmonics**
s-Polarized Fundamental	Odd	Even
p-Polarized Fundamental	None	Odd and Even

2.2.1.2 HHG Spectrum

We chose the coordinate system shown in Fig. 4. The incident light is polarized along the y-axis. The electric field of the incident light is given by:

$$E(t, x, z) = E_0 \exp\left(-i\omega_0 \left(t - x/c \sin\alpha - z/c \cos\alpha\right)\right)$$

We assume the surface oscillations to be of the form:

$$s(t) = s_0 \sin\left(\omega_m \left(t - x/c \sin\alpha\right)\right)$$

The maximum displacement of the surface is s_0 is limited by the condition that the velocity must not exceed the speed of light. For example, for s-polarization, as $\omega_m = 2\omega_0$, we have

$$s_0 < \frac{c}{\omega_0} = \frac{c}{2\omega_0}$$
$$\therefore \chi < \cos\alpha$$

We assume that the reflected wave can be written in the general form of a plane wave propagating in the specular direction:

$$E_R = G(u) = G(t - x/\sin\alpha + z/\cos\alpha)$$

If we further assume that the surface is completely reflecting, then $G(u)$ is obtained from the condition that the total field must vanish on the reflecting surface $z = s(t, x)$, that is:

$$E(t, x, s(t, x)) + E_R(t, x, s(t, x)) = 0 \tag{5}$$

Both sides of Eq. 5 are a function only of $\xi = t - x/c \sin\alpha$. The spectrum of the reflected wave can be determined using the Fourier transform of $G(u)$:

$$G(\omega) = \int_{-\infty}^{\infty} G(u) e^{-i\omega u} du$$

where $u = \xi - s_0/c \cos\alpha \sin(\omega_m \xi)$ Integrating, this comes out to be:

$$G(\omega) = -2\pi E_0 \sum_{-\infty}^{+\infty} \frac{1}{1 + n\omega_m/2\omega_0} \times J_n\left(\left(1 + n\omega_m/2\omega_0\right)\xi\right) \delta\left(\omega - \omega_0 - n\omega_m\right) \tag{6}$$

where J_n are the Bessel functions of order n.

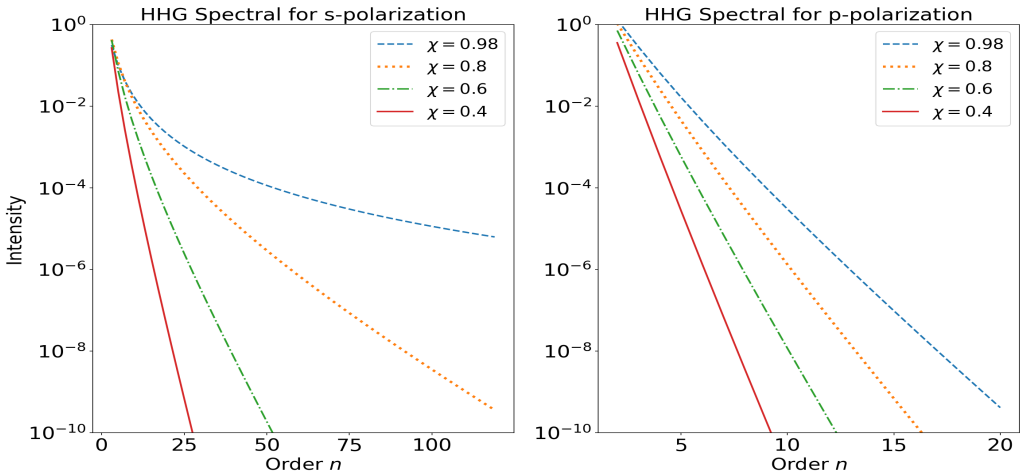

Figure 5: HHG spectrum for s and p polarization. The amplitudes of HHG is decreasing more rapidly for p-polarization than s-polarization

For an s-polarization we have, $\omega_m = 2\omega_0$ and hence equation 6 reduces to:

$$S((2n+1)\omega_0) = (\pi E_0)^2 \left(\frac{J_n((n+1)\xi)}{(n+1)} - \frac{J_{n+1}(n\xi)}{(n)} \right)^2 \tag{7}$$

For a p-polarization:

$$S(n\omega_0) = (\pi E_0)^2 \left(\frac{J_{n-1}(\frac{1}{2}(n+1)\xi)}{\frac{1}{2}(n+1)} - \frac{J_{n+1}\frac{1}{2}((n-1)\xi)}{\frac{1}{2}(n-1)} \right)^2 \tag{8}$$

A plot of the spectra is shown in figure 5.

2.2.2 Universal Spectra

The *ideal mirror* assumptions made by von der Linde et al.[11] are not held in practice. In fact, an ideal mirror is not physically possible. Gordienko et al.[14] showed that it is not necessary to assume a form of plasma surface oscillation if the goal is just to get the cutoff and power law of the HHG spectrum. Assuming only the boundary condition equation 5 and the periodicity of the surface motion, they found the following results which are valid for any type of plasma surface motion:

1. The power law for monochromatic wave

$$I_n \propto 1/n^{5/2} \tag{9}$$

2. The power law for broadband wave

$$I_n \propto 1/n^{5/2}$$

3. The cutoff

$$n_c \propto 4\gamma_{\max}^2 \tag{10}$$

3 Methodology

3.1 PIC Approach

The present report uses *EPOCH*[15], which is a fully relativistic, 3D, parallelized implementation of the particle-in-cell algorithm. PIC is a numerical approach that simulates a collection of particles that interact via external and self-induced electromagnetic fields. A spatial grid is used to describe the field while the particles move in the continuous space. The field and the particle motion are solved concurrently. In this way the simulation requires less amount of work, since each particle only interacts with the grid points of the cell where it is located.

3.2 Simulation Setup

The present report includes two types of simulations: first, we use a normally incident laser pulse to study the effect of SG envelope on the generated HHG. Secondly, we have performed some simulations to study the oblique incidence and different polarization.

3.2.1 For Normal Incident

The simulation box extends for $40\lambda_l$ (from $-20\lambda_l$ to $20\lambda_l$), where λ_l is the laser wavelength taken as $1\mu m$ and has a total of 16000 cells, i.e., 400 cells per wavelength. The plasma is placed at $x = 0$ and with a thickness of λ_l. The number of particles per cell is 100. The pulse duration is $T = 20\tau$ and the simulation is run till $T_{end} = 40\tau$. Here τ is the time period of the laser pulse. The study of SG envelope is performed in the normal incidence. So, the envelope used is SG given by:

$$P = P_0 \exp\left(-2\left(\frac{x-\mu}{\sigma}\right)^p\right) \tag{11}$$

where P_0 is the normalization constant, μ is the mean, σ is the standard deviation and p is the power of the SG.

3.2.2 For Oblique Incident

To report uses only a 1D simulation for oblique incidence. This is accommodated by following Bourdier transformation[16], where simulations are performed in a moving frame in which the light is normally incident. (See figure 6)

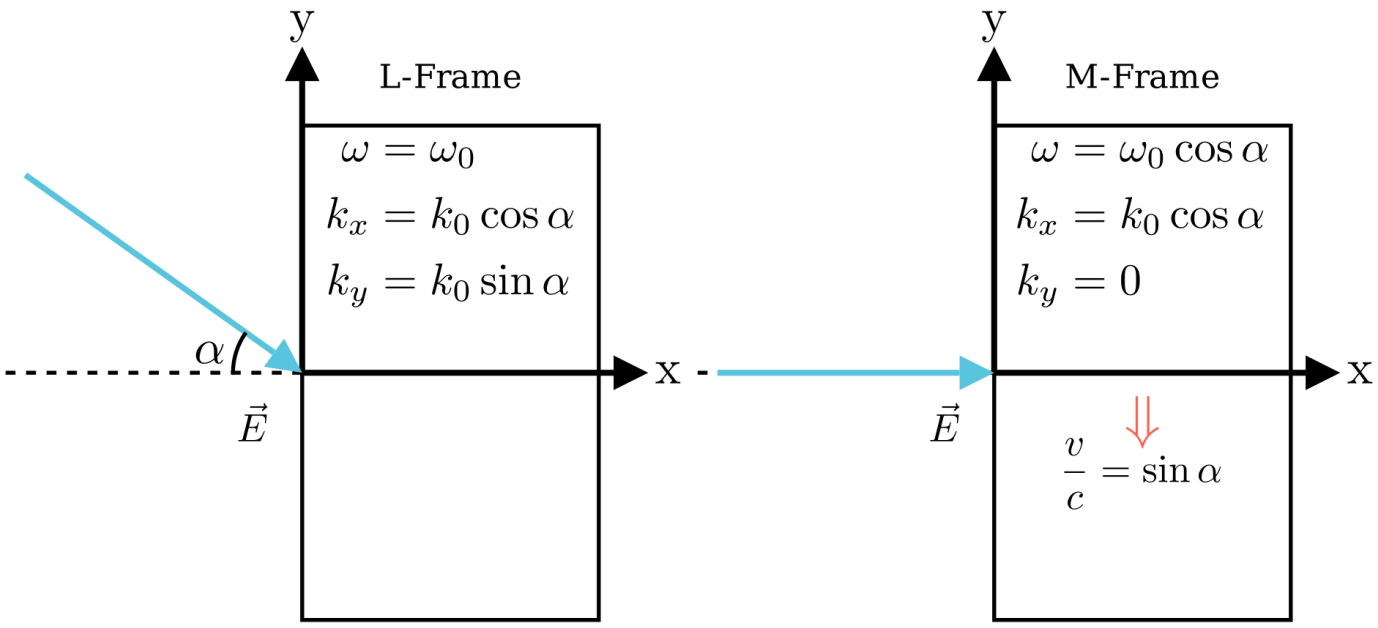

Figure 6: L is the lab frame and M is the moving frame. Simulations are done in the M-frame and then they are transformed back to the L-Frame

To do this, we make a Lorentz transformation from the laboratory frame L to frame M, moving in y direction with a velocity of $\mathbf{v_M} = c\sin\alpha\hat{y}$. This way, the incident pulse is normal to the surface in the M-frame as the figure shows. This makes the plasma to be moving with a velocity of $-\mathbf{v_f}$. The frequency ω_0 and the wave vector $\mathbf{k_0}$ changes so that the speed of light is the same. The transformations of these are in figure 6.

The electric and magnetic field also changes. For p-polarization, the transformation equations are:

$$\begin{aligned} \mathbf{E}_L &= E_0(-\sin\alpha\hat{x} + \cos\alpha\hat{y}) \\ \mathbf{E}_M &= E_0\cos\alpha\hat{y} \\ c\mathbf{B}_L &= E_0\hat{z} \\ c\mathbf{B}_M &= E_0\cos\alpha\hat{z} \end{aligned} \tag{12}$$

While for s-polarization:

$$\begin{aligned} \mathbf{E}_L &= E_0\hat{z} \\ \mathbf{E}_M &= E_0\cos\alpha\hat{z} \\ c\mathbf{B}_L &= E_0(\sin\alpha\hat{x} - \cos\alpha\hat{y}) \\ c\mathbf{B}_M &= -E_0\cos\alpha\hat{y} \end{aligned} \tag{13}$$

Note that the field amplitudes are decreased by a factor of $\cos\alpha$ and hence intensity also decreases. However, the normalized vector potential $a_0 = eE_0/m\omega_0 c$ remains invariant. The density becomes $n_M = n_0/\cos\alpha$. A summary of these transformations is given in the table below:

Table 2: Transformation Equations

Quantity	**L-Frame**	**M-Frame**
ω	ω_0	$\omega_0\cos\alpha$
λ	λ_0	$\lambda_0/\cos\alpha$
n	n_0	$n_0/\cos\alpha$
E (p-polarized)	$E_0(-\sin\alpha\hat{x} + \cos\alpha\hat{y})$	$E_0\cos\alpha\hat{y}$
E (s-polarized)	$E_0\hat{z}$	$E_0\cos\alpha\hat{z}$
B (p-polarized)	$E_0\hat{z}$	$E_0\cos\alpha\hat{z}$
B (s-polarized)	$E_0(\sin\alpha\hat{x} - \cos\alpha\hat{y})$	$-E_0\cos\alpha\hat{y}$

4 Summary of Work Done in the Previous Semester

We started by doing simulations using the particle-in-cell algorithm to study the laser-plasma interaction. We varied laser intensity and plasma density to study the reflection of the laser from plasma. We verified that the laser is reflected from overdense plasma, while underdense plasma acts as a transparent medium. We also investigated how plasma surface oscillation varies with changes in plasma density and laser intensity. Additionally, we observed that altering the laser intensity resulted in changes in the *apparent* critical density of the plasma.

Our interest then shifted toward the study of high harmonic generation. This process involves the interaction between laser and plasma, which results in the generation of higher frequency harmonics of the incident laser radiation. To investigate this phenomenon, we performed a series of simulations, focusing on how various plasma and laser parameters affect the generated high harmonics. Our simulations involved examining the effects of parameters such as plasma density, laser intensity, laser envelope, and laser pulse length on high harmonic generation. In addition to our study of plasma and laser parameters, we also extended our investigation to include the study of surface oscillation. Specifically, we aimed to understand the frequency of these oscillations and how they relate to the generation of high harmonics. Through our simulations, we found that only odd harmonics are generated in the reflected wave under

normal incidence, while even harmonics are generated through the oscillation of the surface. We also observed a resonance at $n_0/n_c = 4$. We found that the envelopes had no significant effect on HHG while increasing laser intensity increases the number of harmonics generated as well as their amplitude.

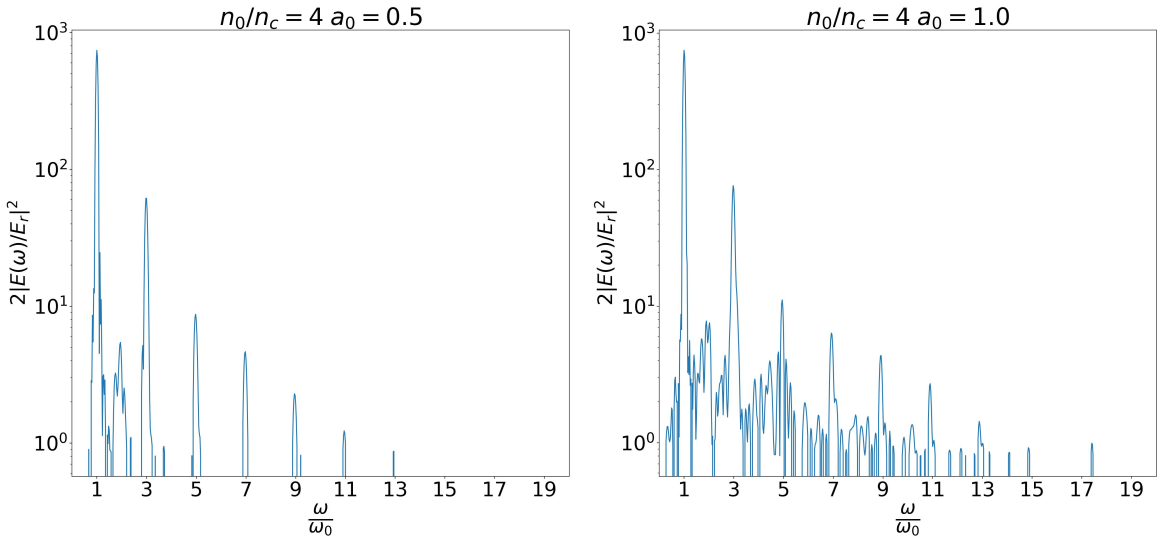

Figure 7: The spectrum shows that only odd harmonics are generated. The number of harmonics and their intensity increases with an increase in normalized vector potential a_0

5 Results and Discussion

5.1 Super-Gaussian Envelope

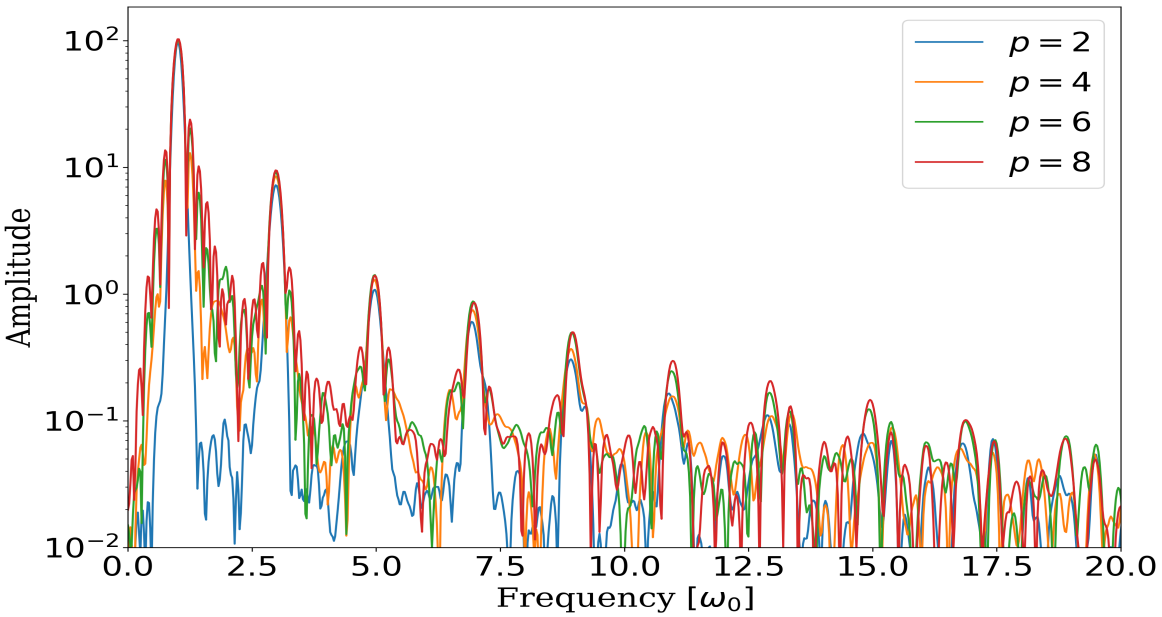

Figure 8: The spectrum of SG envelopes with power 2,4,6, and 8 are shown in a single plot. A small increase in the peak amplitude is observed with increasing power.

The SG envelope, given by equation 11 has a different area for different p and hence has different energy for the same given intensity. To mitigate this, the simulation is performed by multiplying the given intensity of the pulse such that the total energy of all the pulses is the same. This is done by taking a reference SG beam (we have used $p = 2$), evaluating its area and then normalizing the intensities of other SG pulses by the ratio of this reference area and the area of the corresponding SG envelope. The spectrum of the HHG generated using laser pulse with SG envelopes with power 2, 4, 6, and 8 are shown in figure 8. It is observed that a small increase in the amplitude is followed by increasing power of the SG envelope.

5.2 p-Polarization

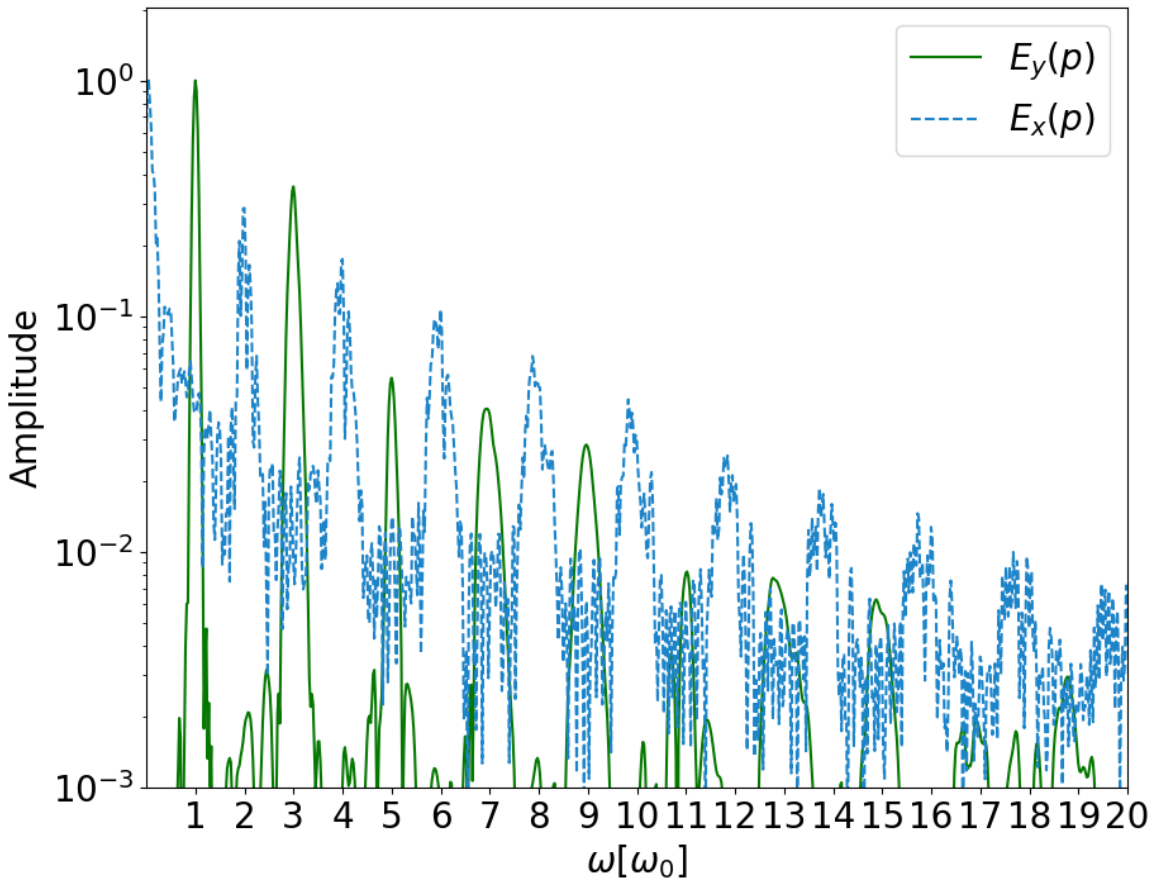

Figure 9: The spectrum of HHG for p-polarized light. Simulation parameters are $\alpha = \pi/4$, the density is $n_0 = 7n_c$ and $a_0 = 4$

Figure 9 shows the spectrum of HHG in the L-frame, when p-polarized light is incident on the plasma. As discussed in section 2.3.1.1 (see that table 1), the spectrum is made up of even and odd p-polarized harmonics. There are no s-polarized harmonics.

5.3 s-Polarization

The L-frame spectrum of HHG is depicted in diagram 10, with plasma being exposed to s-polarized light. As explained in section 2.3.1.1 (see that table 1), the spectrum comprises odd s-polarized har-

monics and even p-polarized harmonics.

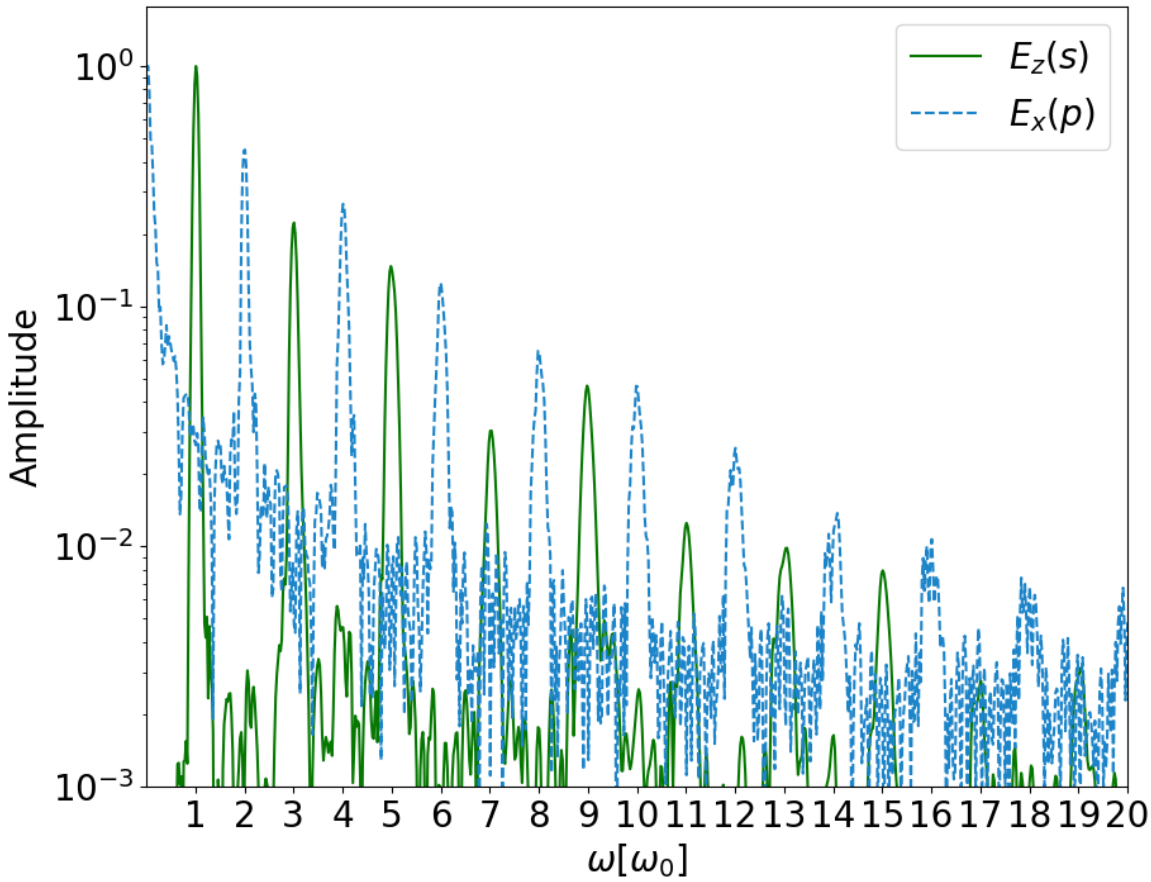

Figure 10: The spectrum of HHG for s-polarized light. Simulation parameters are $\alpha = \pi/4$, the density is $n_0 = 7n_c$ and $a_0 = 4$

6 Future Plan of Work

We plan to continue our research on high harmonic generation. Up till now, we have performed just 1D simulations. We plan to extend our simulations to 2D so that we can compare the results of the oblique incident in 1D to that of 2D.

7 Acknowledgment

We would like to extend our sincerest gratitude to Professor Vikrant Saxena for his unwavering support, patience, motivation, enthusiasm, and invaluable guidance. His mentorship and leadership have been instrumental in the success of this project, and we feel incredibly fortunate to have had the opportunity to work with him.

References

[1] Jin Woo Yoon et al. "Realization of laser intensity over 1023 W/cm2". In: *Optica* 8.5 (May 2021), pp. 630–635. DOI: 10.1364/OPTICA.420520. URL: https://opg.optica.org/optica/abstract.cfm?URI=optica-8-5-630.

[2] Henri Vincenti. "Achieving Extreme Light Intensities using Optically Curved Relativistic Plasma Mirrors". In: *Physical Review Letters* 123.10 (Sept. 2019). DOI: 10.1103/physrevlett.123.105001. URL: https://doi.org/10.1103%2Fphysrevlett.123.105001.

[3] R. Lichters, J. Meyer-ter-Vehn, and A. Pukhov. "Short-pulse laser harmonics from oscillating plasma surfaces driven at relativistic intensity". In: *Physics of Plasmas* 3.9 (1996), pp. 3425–3437. DOI: 10.1063/1.871619. URL: https://doi.org/10.1063/1.871619.

[4] Michael D. Perry and Gerard Mourou. "Terawatt to Petawatt Subpicosecond Lasers". In: *Science* 264.5161 (1994), pp. 917–924. DOI: 10.1126/science.264.5161.917. URL: https://www.science.org/doi/abs/10.1126/science.264.5161.917.

[5] J. J. Macklin, J. D. Kmetec, and C. L. Gordon. "High-order harmonic generation using intense femtosecond pulses". In: *Phys. Rev. Lett.* 70 (6 Feb. 1993), pp. 766–769. DOI: 10.1103/PhysRevLett.70.766. URL: https://link.aps.org/doi/10.1103/PhysRevLett.70.766.

[6] S G Preston and J B Watson. "Generation of a harmonic quasi-continuum from beating laser fields". In: *Journal of Physics B: Atomic, Molecular and Optical Physics* 31.10 (May 1998), p. 2247. DOI: 10.1088/0953-4075/31/10/014. URL: https://dx.doi.org/10.1088/0953-4075/31/10/014.

[7] Misha Yu Ivanov, Michael Spanner, and Olga Smirnova. "Anatomy of strong field ionization". In: *Journal of Modern Optics* 52.2-3 (2005), pp. 165–184. DOI: 10.1080/0950034042000275360. URL: https://doi.org/10.1080/0950034042000275360.

[8] N B Delone and Vladimir P Krainov. "Tunneling and barrier-suppression ionization of atoms and ions in a laser radiation field". In: *Physics-Uspekhi* 41.5 (May 1998), p. 469. DOI: 10.1070/PU1998v041n05ABEH000393. URL: https://dx.doi.org/10.1070/PU1998v041n05ABEH000393.

[9] Kenichi L. Ishikawa. "High-Harmonic Generation". In: *Advances in Solid State Lasers*. Ed. by Mikhail Grishin. Rijeka: IntechOpen, 2010. Chap. 19. DOI: 10.5772/7961. URL: https://doi.org/10.5772/7961.

[10] B. Bezzerides, R. D. Jones, and D. W. Forslund. "Plasma Mechanism for Ultraviolet Harmonic Radiation Due to Intense CO_2 Light". In: *Phys. Rev. Lett.* 49 (3 July 1982), pp. 202–205. DOI: 10.1103/PhysRevLett.49.202. URL: https://link.aps.org/doi/10.1103/PhysRevLett.49.202.

[11] Dietrich von der Linde and Kazimierz Rzazewski. "High-order optical harmonic generation from solid surfaces". In: *Applied Physics B* 63 (Oct. 1996), pp. 499–506. DOI: 10.1007/s003400050115.

[12] Luis Plaja et al. "Generation of attosecond pulse trains during the reflection of a very intense laser on a solid surface". In: *J. Opt. Soc. Am. B* 15.7 (July 1998), pp. 1904–1911. DOI: 10.1364/JOSAB.15.001904. URL: https://opg.optica.org/josab/abstract.cfm?URI=josab-15-7-1904.

[13] Teodora Baeva, S Gordienko, and A. Pukhov. "Theory of high-order harmonic generation in relativistic laser interaction with overdense plasma". In: *Physical review. E, Statistical, nonlinear, and soft matter physics* 74 (Oct. 2006), p. 046404. DOI: 10.1103/PhysRevE.74.046404.

[14] S. Gordienko et al. "Relativistic Doppler Effect: Universal Spectra and Zeptosecond Pulses". In: *Phys. Rev. Lett.* 93 (11 Sept. 2004), p. 115002. DOI: 10.1103/PhysRevLett.93.115002. URL: https://link.aps.org/doi/10.1103/PhysRevLett.93.115002.

[15] T D Arber et al. "Contemporary particle-in-cell approach to laser-plasma modelling". In: *Plasma Physics and Controlled Fusion* 57.11 (Sept. 2015), p. 113001. DOI: 10.1088/0741-3335/57/11/113001. URL: https://dx.doi.org/10.1088/0741-3335/57/11/113001.

[16] A. Bourdier. "Oblique incidence of a strong electromagnetic wave on a cold inhomogeneous electron plasma. Relativistic effects". In: *The Physics of Fluids* 26.7 (1983), pp. 1804–1807. DOI: 10.1063/1.864355. URL: https://aip.scitation.org/doi/abs/10.1063/1.864355.